

Research Article

Sonochemical Preparation and Subsequent Fixation of Oxygen-Free Graphene Sheets at N,N-Dimethyloctylamine-Aqua Boundary

Elena A. Trusova¹, Klara V. Kotsareva,¹ Alexey N. Kirichenko,² Sergey S. Abramchuk,³ and Igor A. Perezhogin^{2,3,4}

¹Institution of the Russian Academy of Sciences, A.A. Baikov Institute of Metallurgy and Materials Science of RAS, Leninsky Prospect 49, Moscow 119334, Russia

²Technological Institute for Superhard and Novel Carbon Materials, Tsentralnaya Street 7a, Troitsk, Moscow 142190, Russia

³Lomonosov Moscow State University, Leninskie Gory, Moscow 119991, Russia

⁴Moscow Institute of Physics and Technology State University, Institutskiy Per. 9, Dolgoprudny, Moscow Region 141700, Russia

Correspondence should be addressed to Elena A. Trusova; trusova03@gmail.com

Received 10 July 2017; Accepted 10 October 2017; Published 24 January 2018

Academic Editor: Renal Backov

Copyright © 2018 Elena A. Trusova et al. This is an open access article distributed under the Creative Commons Attribution License, which permits unrestricted use, distribution, and reproduction in any medium, provided the original work is properly cited.

In this study, the syntheses of oxygen-free graphene sheets and the method of its fixation at an oil-aqua interface were presented. The graphene sheets were prepared by exfoliation of synthetic graphite powder in an aqua-organic medium under ultrasound irradiation. N,N-Dimethyloctylamine- (DMOA-) aqua emulsion was used as the liquid medium, and pH was equal to 3. The obtained graphene nanosuspension was fractionated by sedimentation and decanted according to the weight. The graphene nanoparticle fractions, differing in configuration and number of layers, have been characterized using transmission electron microscopy (TEM), electron diffraction, HRTEM, Raman spectroscopy, and electron energy loss spectroscopy (EELS). It was found that using a DMOA-aqua mixture as the liquid medium in ultrasonic treatment of synthetic graphite leads to the formation of oxygen-free 1-2-layer graphene sheets attached to the DMOA-aqua interface. The proposed method differs from known ones by using a small amount of more environmentally friendly organic substances. It allows to obtain large quantities of oxygen-free graphene, and finally unconverted graphite can be directed for reuse. The proposed method allows to obtain both 2D graphene sheets with micron linear dimensions and 3D packages with a high content of defects. Both these species are in demand in areas related to the development of new materials with unique electrophysical properties.

1. Introduction

In recent years, researchers and developers have shown great interest in 2D and 3D graphene, which is required for production of new raw materials that are in demand by production of sensors, new generation electronic devices, and energy storage [1–8]. All these materials are needed for a variety of industries: noncarbon energetics, automotive, robotics, creating of the drones, new materials for aerospace and military sectors [9–12]. Creation of cost-effective technologies for the production of sufficient quantities of high-quality raw materials requires the development of

efficient and environmentally friendly methods of graphene sheet exfoliation. Lately, the method of ultrasonic liquid media exfoliation of graphene sheets from a graphite surface is recognized as the most technologically acceptable [13–16]. Among solution phase exfoliation techniques, the aqueous-based exfoliation of graphite is one of the most promising ways to mass produce graphene at extremely low cost and minimal environmental impact [13, 17].

The unique electronic, thermal, and mechanical properties of 2D and 3D graphene species are caused by their structure, formed by layers of sp^2 carbon atoms linked by covalent bonds in 5- and 6-membered rings [18–20].

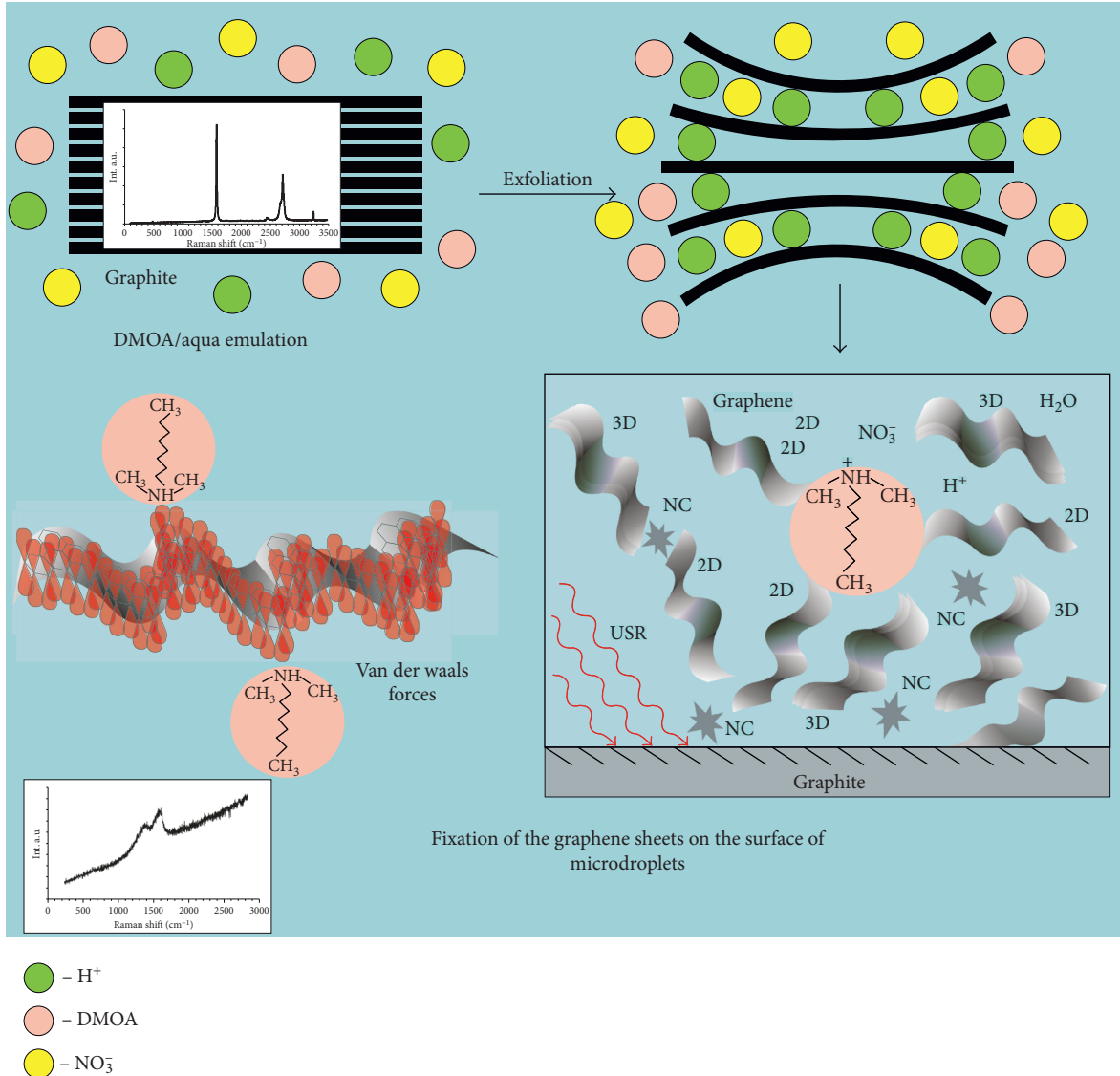


FIGURE 1: Mechanism for the formation of graphene by exfoliating graphite powder and its fixation on the surface of DMOA nanodroplets in acidified aqua-oil emulsion. NC: nanocarbon; USR: ultrasonic radiation.

Typically, in most cases, graphene converts into graphene oxide in contact with oxygen as a result of transition of sp^2 carbon atoms into sp^3 state that impairs the electrical properties of materials [21, 22]. Conversion of graphene to graphene oxide is an irreversible process, and it is impossible to return an original structure and the electrical properties by reduction, the product of which is called a reduced graphene oxide [23]. For these reasons, the development of quantitative methods for the preparation of graphene is the subject of much research in the last few years [15, 17, 23–25].

Alongside the mechanical cleavage based on the scotch tape approach, the liquid-phase exfoliation methods become more and more interesting because they are versatile and potentially upscalable and can be used to deposit graphene in the different mediums on the different substrates, which is impossible using mechanical cleavage. An exfoliation of graphene sheets is carried out by the impact of ultrasound on graphite, and as a result, graphene sheets peel off from

a graphite surface and move into the liquid medium—most often aqua, wherein medium pH value was varied from acidic to alkaline [26]. The different organic substances [18, 22, 27, 28] are used for stabilization of the graphene sheets and prevent their agglomeration. For example, exfoliation of graphene sheets was carried out in the aqueous solutions of alkaline lignin [22], sodium dodecyl sulfate [29], and sodium dodecylbenzene sulfonate [13], as well as in organic solutions of imidazole [30], 1-pyrenecarboxylic acid [31], dimethylformamide [32], mixture of benzene and hexafluorobenzene [16], or heptane [33], as well as the products of polymerization of styrene and divinylbenzene [34].

The utilization of pristine graphene in composite materials would be advantageous due to the cost, but not due to the environmental impact of chemical modification, additional processing steps, and degraded properties [23, 34–36]. In review [37], the authors conclude that the use of traditional solvents, such as perylene-based

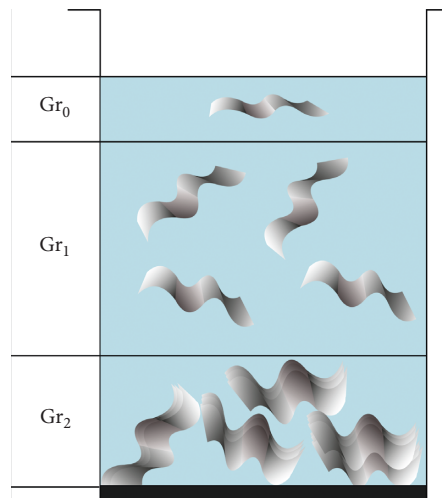


FIGURE 2: Stratification of a graphene suspension and its stepped decantation zones.

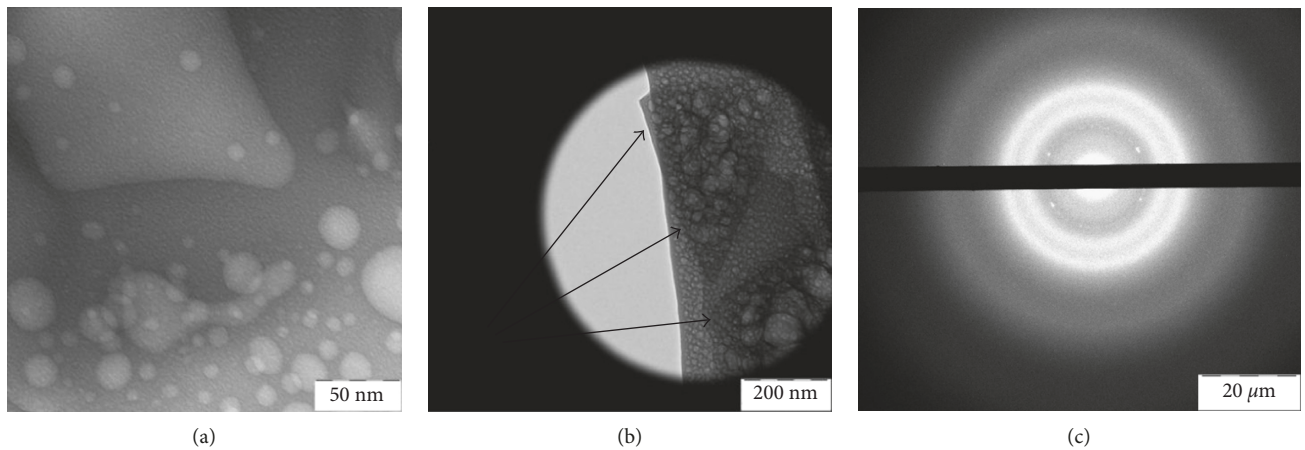


FIGURE 3: TEM images of (a) the organic dispersed (Gr_0) phase in the DMOA-aqua colloid consisted of droplets with partial dark coating and (b) the thick sheets, inside of which the cavities from dispersed phase droplets were kept. (c) Electron diffraction pattern.

bolaamphiphiles, 7,7,8,8-tetracyanoquinodimethane, and coronene tetracarboxylic acids or pyrene-based hydrophilic dendrones, acetonitrile, and melamine additives for stabilization of the aqueous graphene suspensions is problematic due to their toxicity. Therefore, the search for a new liquid-phase system for efficient quantitative exfoliation of the graphene sheets is necessary [28]. However, the knowledge about the surfactant-assisted liquid phase exfoliation of graphite in organic solvents is still relatively poor [38–41]. In order to differentiate a single or two-layer and multilayer graphene sheets, it has been proposed to use the ratio value of the I_{0110}/I_{1210} reflex intensities in electron diffraction pattern [42]. It was found that the appearance of moiré patterns on the surface of graphene nanoparticles on the TEM images is the result of periodic modulations (superstructure) on the surface of graphene with a small disorientation of the surface layers ($1\text{--}9^\circ$) and interaction of two π -electron systems of neighboring layers [43–46].

3D graphene networks are of particular interest to developers of new materials for energy applications due to

high specific surface areas, large pore volumes, strong mechanical strengths, and fast mass and electron transport [47–49]. In the same time, obtaining 3D graphene particles as versatile building blocks for bottom-up assembly of advanced functional materials is a very difficult problem, according to many researchers [50–52]. The development of cost-effective method for producing 2D and 3D graphene stacks with specified dimensions is promising for obtaining van der Waals heterostructures containing different semiconductors in the interlayer space [53, 54]. The noncovalent solution-phase methods are needed to produce oxygen-free graphene, and one such versatile and scalable method is exfoliation in liquid medium with use the organic compounds as solvents, for example, pyrrolidone derivatives, (perfluorocarbocyclic and heterocyclic hydrocarbons, and some oxygenates [27, 55–61].

This paper presents the results of study on exfoliation of oxygen-free graphene from graphite in the N,N-dimethyloctylamine (DMOA)-in-aqua emulsion under ultrasound irradiation followed by fixation of the formed

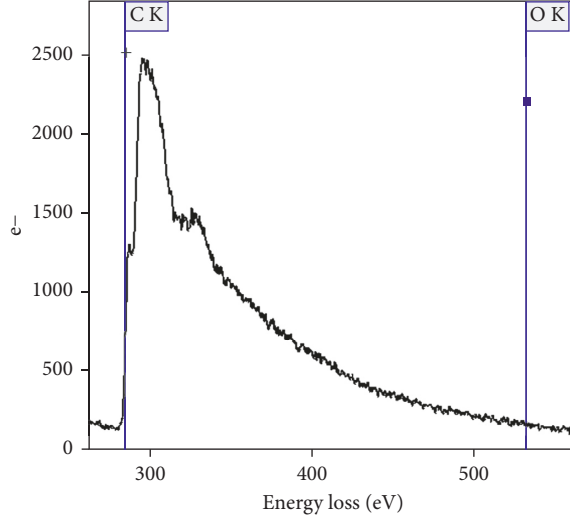


FIGURE 4: EEL spectrum of the Gr_0 fraction, in the range of 250–550 eV, covering C K and O K edges (indicated by vertical lines with markers).

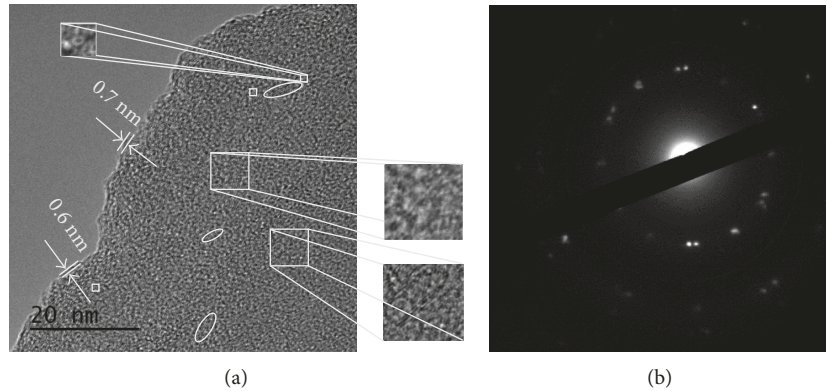


FIGURE 5: (a) HRTEM image of a dried lightest fraction of graphene suspension obtained from the decanted liquid substance after graphene-containing colloid sedimentation during 12 hrs (Gr_0). Inset is a magnified part of the image taken from the regions enclosed by the white squares (not to scale); it shows graphene hexagons. The ovals note 1- and 2-layer graphene flakes. (b) Electron diffraction pattern.

sheets at the phase boundary, which is the surface of DMOA microdroplets. The proposed method also differs from others by the mild conditions. There is no need to use high temperatures and pressures, which are typical for the solvothermal process. This method of quantitative obtaining of graphene compares favorably with published preparative ones. (1) It is more environmentally friendly, since not using O- and N-containing cyclic compounds having a negative impact on the genetic system of staff working with them; (2) only water is used as solvent, and DMOA only creates an emulsion. Furthermore, this method is a cost-effective on energy, as low temperatures and short ultrasound exposure are used. The developed process does not require much energy for DMOA removal during heat treatment due to its not too high boiling point compared to oleylamine, used as a solution in environmentally unfriendly chloroform [56, 62, 63]. The graphene nanoparticles fractions, differing in configuration and number of layers, were characterized by using TEM, HRTEM, electron diffraction, and EELS. The

obtained graphene species in the form of 3D stacks self-assembled of 1-2-layer sheets is a promising semiproduct for the materials with strengthened charge transfer and high storage capacity due to the high defect density [64–66].

2. Experimental Section

2.1. Synthesis of Graphene Sheets. In the present work, the graphene sheets were obtained by exfoliation from a surface of powdery synthetic graphite (produced by Processing Science, Russia) in a liquid medium under the ultrasonic exposure. The initial graphite powder had a particle size of 600–800 microns and a purity of 99.99%, while the impurities presented as sulfur (less than 10 ppm) and chloride ions (10 ppm). A batch of graphite powder was mixed with deionized water produced in a reverse osmosis Raifil system. DMOA was used for stabilization of graphene suspension, and DMOA/aqua volume ratio was 1/10. The ultrasound treatment of graphite powder in an organic-aqueous medium was carried out with

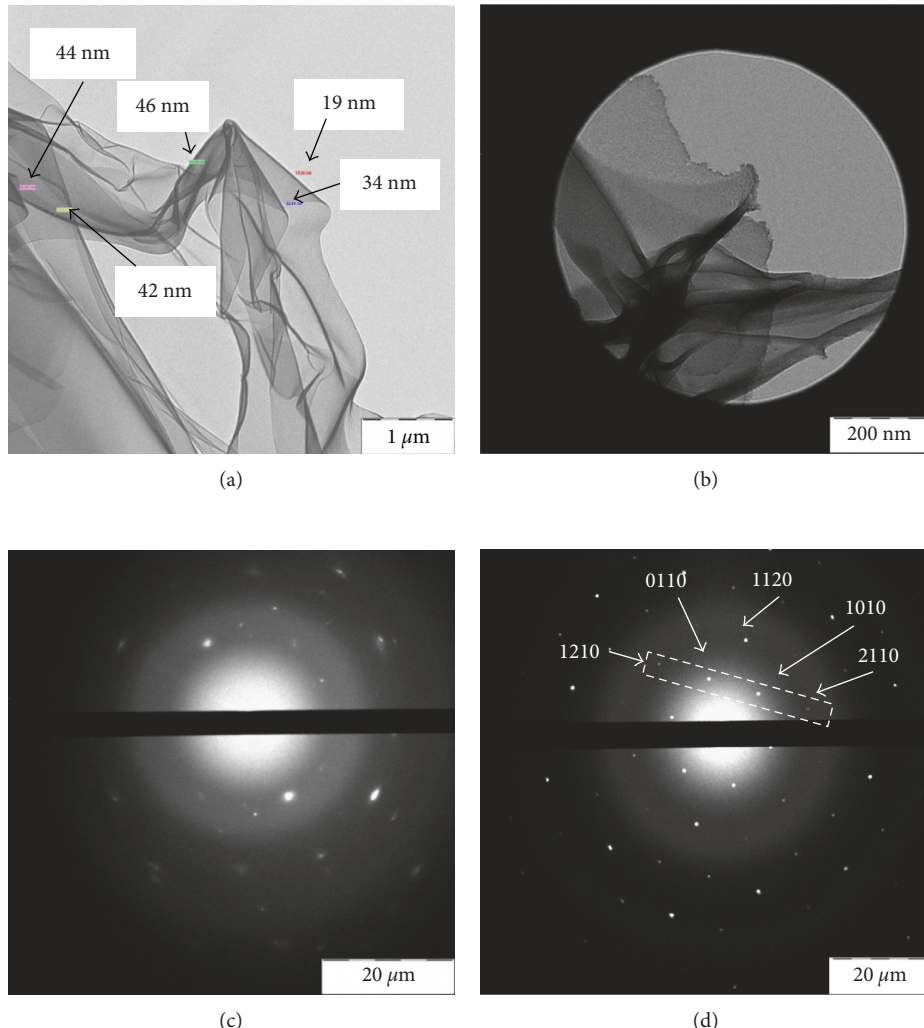


FIGURE 6: (a, b) TEM microphotos (in the bright and dark fields, accordingly) of graphene films obtained from the decanted liquid substance after graphene-containing colloid sedimentation during 12 hrs (Gr₁ fraction). (c, d) Electron diffraction patterns for the different regions of the sample.

air in Sonoswiss SW1H ultrasonic bath with power 200 W at a temperature of the liquid phase about 60°C. The duration of ultrasonic treatment of graphite was 10 hrs. The pH value of the medium was equal to 3 by adding HNO₃.

2.2. Graphene Species Characterization. The obtained fractions of graphene nanoparticles differing in configuration and number of layers have been characterized using TEM, HRTEM, Raman spectroscopy, electron diffraction, and EELS. TEM and selected area electron diffraction studies of obtained graphene species were carried out with use of the LEO-912 AB OMEGA electron microscope operating at 100 kV. HRTEM and EELS data were obtained on the JEM 2010 instrument (JEOL Ltd.) equipped with energy dispersive spectrometry (EDS; Inca, Oxford Instruments) and electron energy loss spectrometry (EELS; GIF Quantum, Gatan Inc.) attachments; accelerating voltage was 160 kV. The thickness and the number of layers in the flakes were calculated based on 5–10 measurements on each of 5–6 TEM

or HRTEM microphotos for each graphene suspension sample. The Raman spectra were excited by 0.5145 nm laser radiation at room temperature and recorded using a Raman spectrometer on the basis of the TRIAX-552 spectrograph with a confocal microscope and a SPEX10 TE-cooled CCD camera: 2kBUV with the spectral resolution of 1 cm⁻¹.

3. Results and Discussion

Usually, exfoliation results in the formation of 2D sheets consisting from 1 to 10 layers as well as 3D sheets, which include more than 10 differently oriented graphene layers. DMOA was used for the stabilization of obtained graphene suspension and the formation of oil-in-aqua emulsion, in which separated graphene sheets were fixed on the DMOA microdroplets' surface due to van der Waals forces [67]. The choice of DMOA is determined by the fact that its volumetric and mobile HC fragment creates significant steric hindrances for the consolidation and compaction of the graphene particles and reconstruction of graphite structure.

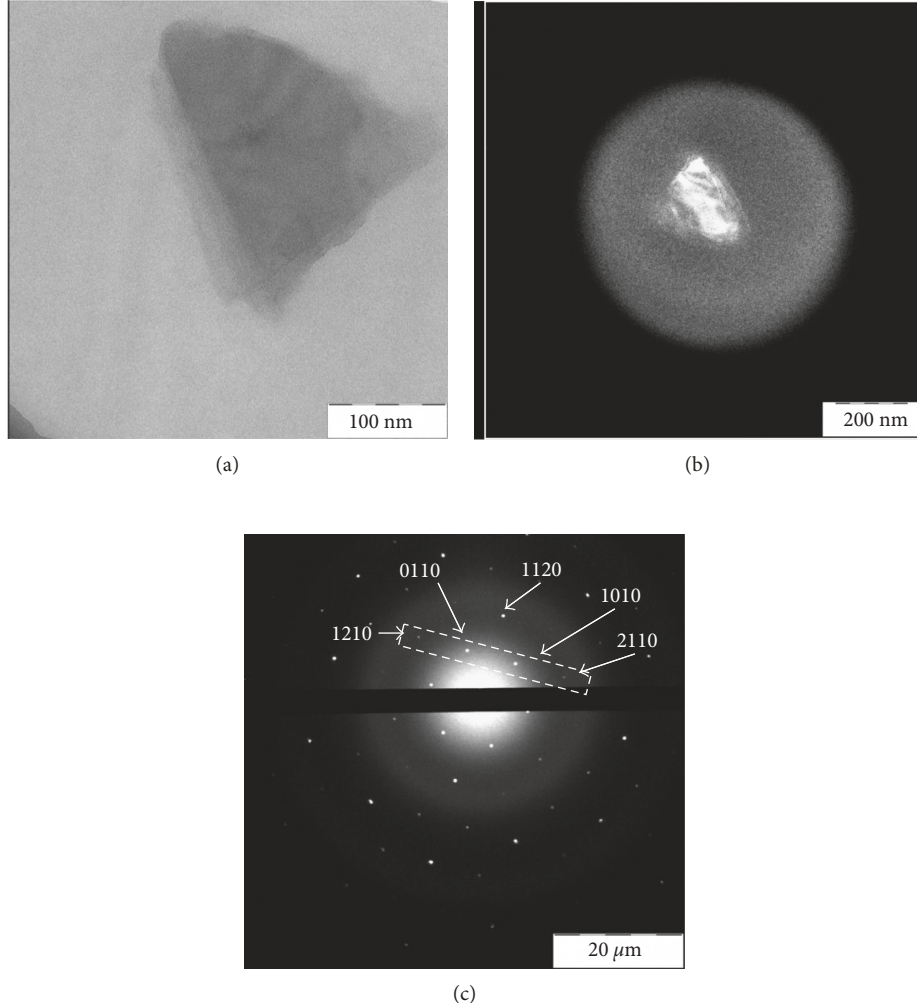


FIGURE 7: TEM images of graphene clusters from the Gr_2 fraction. (a) Bright-field shooting. (b) Dark-field shooting. (c) Electron diffraction pattern.

Figure 1 shows the mechanism for the formation of graphene sheets and their fixation on DMOA droplets' surface in the acidified oil-in-aqua emulsion. The surfactant-assisted liquid-phase process of obtaining a graphene suspension from graphite powder involves 3 steps: (1) swelling of surface graphite layers in an acid medium under ultrasonic irradiation (USR) and exfoliation of the carbon layers from the graphite particles, (2) dispersion of obtained surfactant-coated graphene sheets in an exfoliating medium, and (3) stabilization of a resulting suspension. The first stage begins with the attack of nitrate ions to the edge sites of graphite particles, and then, the intercalation of nitrate ions occurs into graphite interlayer spacing followed by its expansion [37, 68]. During this stage, the water molecules may cointercalate with the nitrate anions, and as a result, a detachment of graphene sheets occurs.

In the second stage, quaternary (protonated) nitrogen atoms of DMOA molecules and sp^2 carbon atoms of graphene sheets interact via the Coulomb force [69, 70], and the formed associates are removed from the graphite surface to the exfoliating medium by the “sliding” mechanism. Finally, in the third step, graphene colloid stabilization takes place due

to fixation of the carbon sheets on the surface of DMOA nanodroplets by van der Waals interaction. Herewith, a partial self-assembly combination of some 1-2-layer sheets occurs with the formation of covalent carbon bonding between the separate graphene sheets. DMOA accelerates the physical binding of graphene sheets by interacting of their sp^2 -electrons with the quaternary ammonium cation and promotes the removal of graphene sheets from exfoliation region to liquid substrate. For comparison, the insets show Raman spectra of the original synthetic graphite and graphene prepared with a high concentration of defects (Figure 1).

After 12 hr sedimentation, the stabilized graphene suspension was decanted to obtain three fractions: light (Gr_0), middle (Gr_1), and heavy (Gr_2), which were investigated differentially (Figure 2).

Figures 3(a) and 3(b) show that an organic dispersed phase in the aqua-DMOA colloid consisted of droplets with partial dark coating. A droplet's diameter was from several nanometers to 50 nm wherein the predominant particle sizes were 15–30 nm. Electron diffraction pattern (Figure 3(c)) corresponds to 1-2-layer graphene. Apparently, graphene supracolloidal structures were absorbed onto the surface of

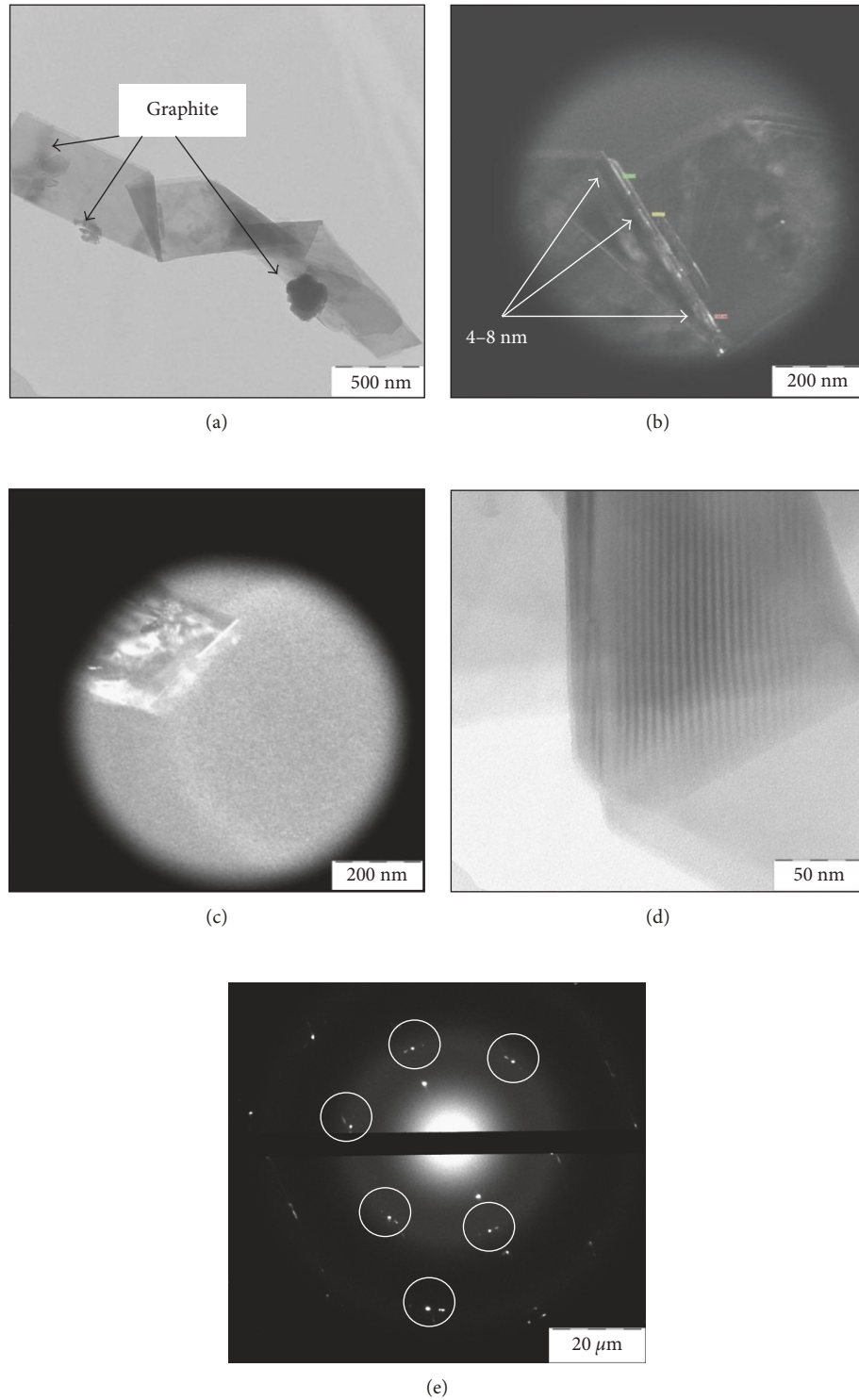


FIGURE 8: TEM images of the Gr_2 fraction. (a) The tape with graphite particles, retaining it. (b) Dark-field microphoto of the graphene tape bending region. (c) Dark-field microphoto of graphene tape edge with moiré. (d) 3D stack. (e) Electron diffraction pattern (the circles indicate reflexes doublets).

dispersed phase droplets as in Pickering emulsions [71] and keep the droplets contour after their drying.

As a result, the thin sheet layers were formed on the DMOA-aqua interface and repeated the dispersed droplet forms. The drying of samples in the preparation mixing occurs

simultaneously with the formation of a graphene layer that follows the dispersed droplets contours. In addition to the coating of the dispersed colloidal particles, graphene also presented as thick 3D sheets, inside of which the cavities from dispersed phase droplets were kept (Figure 3(b)).

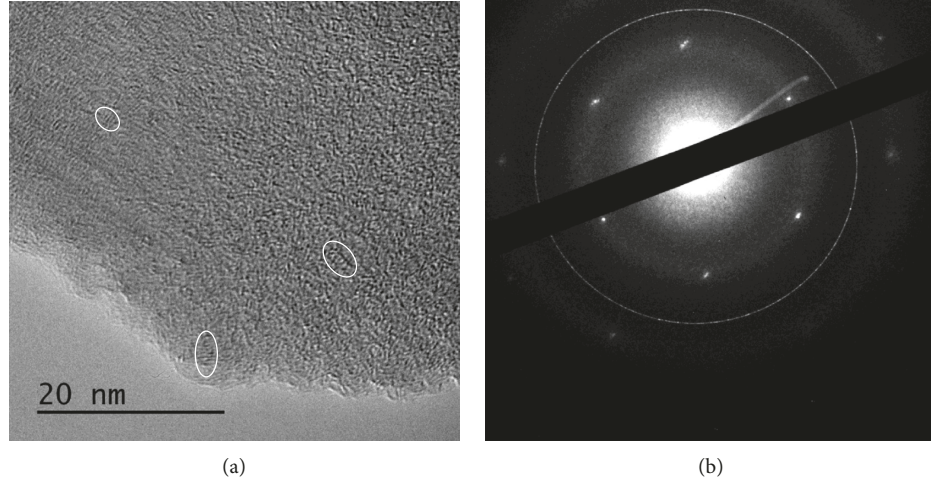


FIGURE 9: (a) HRTEM image of the Gr_2 fraction (some 3D stacks are highlighted with ovals). (b) Electron diffraction pattern.

According to EELS analysis, graphene oxide was absent in the obtained graphene (Gr_0): 532 eV peak corresponding to oxygen does not appear in the spectrum (Figure 4). At the same time, peak at 284 eV corresponds to $1s \rightarrow \pi^*$ transition [72], denoting the presence of $\text{C}_{\text{sp}2}$.

The obtained graphene was also characterized by HRTEM using a support for application of a suspension drop. A lot of sheets were folded, making it possible to count the number of layers in the image shown in Figure 5(a). It can be seen a wide distribution in linear sizes of graphene nanoparticles (1–6 nm), which are randomly fixed on the support. Due to the folded structure of graphene sheet edges, it is possible to evaluate the thickness of graphene layer. The layer thickness was about 0.6–0.7 (± 0.1) nm, that in accordance with the previously published data [19, 73] corresponds to 1–3 layer graphene, and the majority of sheets consist of 2–5 layers (Figure 5(a)). Herewith, the interlayer distance was less than 0.5 nm, indicating an absence of the modified atoms or groups [73]. These results are confirmed by electron diffraction pattern (Figure 5(b)), which corresponds to the set of differently oriented 2–3-layered nanoparticles.

Figures 6(a) and 6(b) show TEM microphotos of the graphene films obtained from the decanted liquid substance after graphene-containing colloid sedimentation during 12 hrs (Gr_1). As the result of drying on a polymer substrate of the TEM spectrometer, they were attached to one side edge of the support grid (Figures 6(a) and 6(b)), possibly due to statics [42]. The layer thickness measured at bends (Figure 6(a)) corresponds to 12–36 monolayers of graphene. The films had not a planar configuration and took the form of randomly deformed layers, which increases their thermodynamic stability by minimizing the surface energy at room temperature.

The random bends of the film are caused probably by its variable thickness and defects randomly distributed in the layers [74, 75]. The electron diffraction pattern shows multidirectional orientation of the layers, the absence of their preferred orientation in the film, and their variable thickness (Figure 6(c)). However, also observed were areas of single-layer graphene (Figure 6(d)) to which the

reflection intensity ratio values correspond to $I_{\{1010\}}/I_{\{2110\}} > 1$ and $I_{\{0110\}}/I_{\{1210\}} > 1$.

Figures 7(a) and 7(b) show the microphotos of graphene clusters from the Gr_2 fraction with side size about 200 nm, electron diffraction pattern of which corresponds to the hexagonal crystal lattice (Figure 7(c)). Figure 7(b) shows the moiré pattern, indicating that, in this block, individual sheets are so distant from each other, that do not interact, but they create the conditions for modulation of vibrations of one carbon atom layer by closest neighboring layer.

As known [19], this effect is caused by displacement of one graphene layer relative to the other by a certain angle due to the mutual repulsion of sp^2 electron orbitals. The calculation showed that formed hexagonal superstructure has the lattice constant equal to 1.98 Å. In the electron diffraction pattern (Figure 7(c)), the reflection intensity ratio value was $I_{\{1120\}}/I_{\{2110\}} > 1$ which corresponds to monolayer graphene [44, 76].

The heavier fraction Gr_2 consists of graphene clusters as tapes having a few rectilinear kinks and total length up to 3 mkm (Figure 8(a)). The TEM microphoto shows the several graphite nanoparticles with sizes ranging from a few to 200 nm, to which these tapes are attached. The thickness of these tapes near the kinks was 4–8 nm, which corresponds to 6–12 layers (Figures 8(a) and 8(b)). The observed moiré patterns on TEM microphotos indicate that a significant proportion of the layers have the properties of a monolayer (Figure 8(c)).

The regions with a large number of layers are also seen (Figure 8(d)), and electron diffraction pattern confirms this fact (Figure 8(e)). The microphotos (Figures 8(b) and 8(c)) show the tapes with smaller dimensions and different orientations within the graphene layers. Due to this, a significant proportion of the layers are removed from each other at increased distances, which reduces their interplanar interaction. Therefore, a significant proportion of the layers in the film have the properties of 1–2 layers of graphene, which is manifested in the appearance of moiré and in the electron diffraction pattern (Figures 8(b) and 8(c)).

The thickness of the layers within the 3D stacks was $\sim 1.0\text{--}1.1$ (± 0.1) nm.

Furthermore, the multilayer nanoparticles with the dimensions reaching several tens of nanometers were observed in most heavy fraction too (Figure 8(d)). In the latter case, the electron diffraction pattern shows the multiplication of hexagonal pattern (Figure 8(e)) which occurs due to the mechanical stresses that appear during the formation of graphene sheets folds. As a result, the electron density changes, and the probability of electron transitions between neighboring carbon atoms increases, which creates effective electric and magnetic fields within the graphene sheets [77].

HRTEM data of the Gr₂ fraction show that the stacks on instrument substrate are more densely packed and more regularly oriented. 3D stacks with the number of layers more than 3 predominate in this graphene fraction (Figure 9(a)), wherein the thickness of each layer is equal to 1.0 (± 0.1) nm. Electron diffraction pattern also corresponds to the multi-layer graphene with partially disordered arrangement of layers (Figure 9(b)). Thus, electron diffraction and HRTEM data are in agreement.

4. Conclusions

We have developed the synthesis of the oxygen-free graphene sheets with followed their fixation at the DMOA-aqua interface. Graphene sheets were prepared by sonochemical exfoliation of synthetic graphite powder in the organic-aqua medium. A DMOA-aqua mixture was used as the liquid medium, and pH of aqua dispersion medium was equal to 3. The advantages of our approach are due to the fact that, firstly, DMOA was used in the small amounts, and under appropriate conditions of the technological process, its absorption and recycle are possible. Secondly, DMOA is optimal reagent, as it is cheaper than amines with longer hydrocarbon chain. Thirdly, DMOA has the lowest boiling point among the ones with longer hydrocarbon chains, making its removal from the product easier; at the same time, DMOA is less volatile than lighter amines.

The obtained graphene nanoparticles were fractionated by sedimentation and decanting according to the weight. The graphene nanoparticles fractions, differing in configuration and number of layers, have been characterized using TEM, HRTEM, electron diffraction, and EELS. It was found that using a DMOA-aqua mixture in ultrasonic treatment of synthetic graphite leads to the formation of oxygen-free 1-2-layer graphene sheets (2D structure, membrane) attached at the oil-aqua interface. The proposed method differs from the known ones by a small amount of more environmentally friendly used organic substances; it allows to obtain large quantities of oxygen-free graphene, and finally unconverted graphite can be directed for reuse. The proposed method allows to obtain both 2D graphene sheets with micron linear dimensions and 3D packages with a high content of defects. Both these species are in demand in areas related to the development of new materials with unique electrophysical properties.

Conflicts of Interest

The authors declare that they have no conflicts of interest.

Acknowledgments

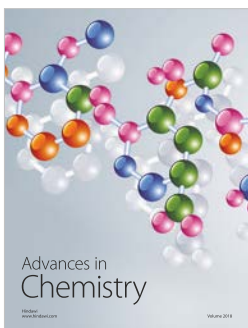
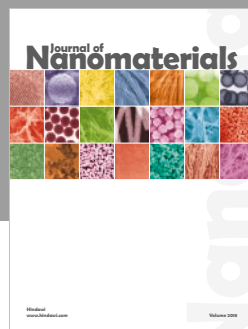
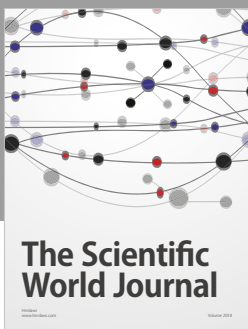
The research was supported by Russian Foundation for Basic Research, Grant no. 17-02-00759_a.

References

- [1] A. K. Geim and K. S. Novoselov, "The rise of graphene," *Nature Materials*, vol. 6, no. 3, pp. 183–191, 2007.
- [2] E. Yoo, J. Kim, E. Hosono, H. S. Zhou, T. Kudo, and I. Honma, "Large, reversible Li storage of graphene nanosheet families for use in rechargeable lithium ion batteries," *Nano Letters*, vol. 8, no. 8, pp. 2277–2282, 2008.
- [3] A. K. Geim, "Graphene: status and prospects," *Science*, vol. 324, no. 5934, pp. 1530–1534, 2009.
- [4] X. Huang, X. Qi, F. Boey, and H. Zhang, "Graphene-based composites," *Chemical Society Reviews*, vol. 41, no. 2, pp. 666–686, 2012.
- [5] H. Jiang, "Chemical preparation of graphene-based nano-materials and their applications in chemical and biological sensors," *Small*, vol. 7, no. 17, pp. 2413–2427, 2011.
- [6] T. Ramanathan, A. A. Abdala, S. Stankovich et al., "Functionalized graphene sheets for polymer nanocomposites," *Nature Nanotechnology*, vol. 3, no. 6, pp. 327–331, 2008.
- [7] C. G. Liu, Z. N. Yu, D. Neff, A. Zhamu, and B. Z. Jang, "Graphene-based supercapacitor with an ultrahigh energy density," *Nano Letters*, vol. 10, no. 12, pp. 4863–4868, 2010.
- [8] W. Du, X. Jiang, and L. Zhu, "From graphite to graphene: direct liquid-phase exfoliation of graphite to produce single- and few-layered pristine graphene," *Journal of Materials Chemistry A*, vol. 1, no. 36, pp. 10592–10606, 2013.
- [9] L. Zhang, F. Zhang, X. Yang et al., "Porous 3D graphene-based bulk materials with exceptional high surface area and excellent conductivity for supercapacitors," *Scientific Reports*, vol. 3, no. 1, p. 1408, 2013.
- [10] S. Han, D. Wu, L. Shuang, Z. Fan, and F. Xinliang, "Porous graphene materials for advanced electrochemical energy storage and conversion devices," *Advanced Materials*, vol. 26, no. 6, pp. 849–864, 2014.
- [11] L. Jiang and Z. Fan, "Design of advanced porous graphene materials: from graphene nanomesh to 3D architectures," *Nanoscale*, vol. 6, no. 4, pp. 1922–1945, 2014.
- [12] X. Cao, Z. Yin, and H. Zhang, "Three-dimensional graphene materials: preparation, structures and application in supercapacitors," *Energy & Environmental Science*, vol. 7, no. 6, pp. 1850–1865, 2014.
- [13] M. Lotya, Y. Hernandez, P. J. King et al., "Liquid phase production of graphene by exfoliation of graphite in surfactant/water solutions," *Journal of the American Chemical Society*, vol. 131, no. 10, pp. 3611–3620, 2009.
- [14] X. Wang, P. F. Fulvio, G. A. Baker et al., "Direct exfoliation of natural graphite into micrometre size few layers graphene sheets using ionic liquids," *Chemical Communications*, vol. 46, no. 25, pp. 4487–4489, 2010.
- [15] M. Lotya, P. J. King, U. Khan, S. De, and J. N. Coleman, "High-concentration, surfactant-stabilized graphene dispersions," *ACS Nano*, vol. 4, no. 6, pp. 3155–3162, 2010.
- [16] A. J. Oyer, J. Y. Carrillo, C. C. Hire et al., "Isotopic-induced variation in the stability of FMN-wrapped carbon nanotubes,"

- Journal of the American Chemical Society*, vol. 134, pp. 5018–5021, 2012.
- [17] U. Khan, A. O'Neill, M. Lotya, S. De, and J. N. Coleman, “High-concentration solvent exfoliation of graphene,” *Small*, vol. 6, no. 7, pp. 864–871, 2010.
- [18] S. Stankovich, D. A. Dikin, G. H. B. Domke et al., “Graphene-based composite materials,” *Nature*, vol. 442, no. 7100, pp. 282–286, 2006.
- [19] J. C. Meyer, A. K. Geim, M. I. Katsnelson, K. S. Novoselov, T. J. Booth, and S. Roth, “The structure of suspended graphene sheets,” *Nature*, vol. 446, no. 7131, pp. 60–63, 2007.
- [20] X. Huang, Z. Yin, S. Wu et al., “Graphene-based materials: synthesis, characterization, properties, and applications,” *Small*, vol. 7, no. 14, pp. 1876–1902, 2011.
- [21] D. W. Boukhvalov and M. I. Katsnelson, “Chemical functionalization of graphene with defects,” *Nano Letters*, vol. 8, no. 12, pp. 4373–4379, 2008.
- [22] W. Liu, R. Zhou, D. Zhou et al., “Lignin-assisted direct exfoliation of graphite to graphene in aqueous media and its application in polymer composites,” *Carbon*, vol. 83, pp. 188–197, 2015.
- [23] S. Pei and H. M. Cheng, “The reduction of graphene oxide,” *Carbon*, vol. 50, no. 9, pp. 3210–3228, 2012.
- [24] J. N. Coleman, “Liquid exfoliation of defect-free graphene,” *Accounts of Chemical Research*, vol. 46, no. 1, pp. 14–22, 2013.
- [25] W. Du, J. Lu, P. Sun, Y. Zju, and X. Jiang, “Organic salt-assisted liquid-phase exfoliation of graphite to produce high-quality graphene,” *Chemical Physics Letters*, vol. 568–569, pp. 198–201, 2013.
- [26] K. B. Ricardo, A. Sendecki, and H. Liu, “Surfactant-free exfoliation of graphite in aqueous solutions,” *Chemical Communications*, vol. 50, no. 21, pp. 2751–2754, 2014.
- [27] A. B. Bourlinos, V. Georgakilas, R. Zboril, T. A. Steriotis, and A. K. Stubos, “Liquid-phase exfoliation of graphite towards solubilized graphenes,” *Small*, vol. 5, no. 16, pp. 1841–1845, 2009.
- [28] A. Ciesielski and P. Samori, “Graphene via sonication assisted liquid-phase exfoliation,” *Chemical Society Reviews*, vol. 43, no. 1, pp. 381–398, 2014.
- [29] C. Yeon, S. J. Yun, K. S. Lee, and J. W. Lim, “High-yield graphene exfoliation using sodium dodecyl sulfate accompanied by alcohols as surface-tension-reducing agents in aqueous solution,” *Carbon*, vol. 83, pp. 136–143, 2015.
- [30] I. W. P. Chen, Y. S. Chen, N. J. Kao, C. W. Wu, Y. W. Zhang, and H. T. Li, “Scalable and high-yield production of exfoliated graphene sheets in water and its application to an all-solid-state supercapacitor,” *Carbon*, vol. 90, pp. 16–24, 2015.
- [31] X. H. An, T. J. Simmons, R. Shah et al., “Stable aqueous dispersions of noncovalently functionalized graphene from graphite and their multifunctional high-performance applications,” *Nano Letters*, vol. 10, no. 11, pp. 4295–4301, 2010.
- [32] V. Georgakilas, K. Vrettos, K. Katomeri et al., “Highly dispersible disk-like graphene nanoflakes,” *Nanoscale*, vol. 7, no. 37, pp. 15059–15064, 2015.
- [33] S. J. Woltonist, A. J. Oyer, J. M. Y. Carrillo, A. V. Dobrynin, and D. H. Adamson, “Conductive thin films of pristine graphene by solvent interface trapping,” *ACS Nano*, vol. 7, no. 8, pp. 7062–7066, 2013.
- [34] H. A. Becerril, J. Mao, Z. Liu, R. M. Stoltberg, Z. Bao, and Y. Chen, “Evaluation of solution-processed reduced graphene oxide films as transparent conductors,” *ACS Nano*, vol. 2, no. 3, pp. 463–470, 2008.
- [35] H. Liu, L. Zhang, Y. Guo et al., “Reduction of graphene oxide to highly conductive graphene by Lawesson’s reagent and its electrical applications,” *Journal of Materials Chemistry C*, vol. 1, no. 18, pp. 3104–3109, 2013.
- [36] S. J. Woltonist and D. H. Adamson, “Properties of pristine graphene composites arising from the mechanism of graphene-stabilized emulsion formation,” *Industrial & Engineering Chemistry Research*, vol. 55, no. 24, pp. 6777–6782, 2016.
- [37] C. H. Chen, S. W. Yang, M. C. Chuang, W. Y. Woon, and C. Y. Su, “Towards the continuous production of high crystallinity graphene via electrochemical exfoliation with molecular in situ encapsulation,” *Nanoscale*, vol. 7, no. 37, pp. 15362–15373, 2015.
- [38] M. S. Kang, K. T. Kim, J. U. Lee, and W. H. Jo, “Large area uniformly oriented multilayer graphene with high transparency and conducting properties derived from highly oriented polyethylene films,” *Journal of Materials Chemistry C*, vol. 1, pp. 1870–1875, 2013.
- [39] J. Geng, B. S. Kong, S. B. Yang, and H. T. Jung, “Preparation of high-quality graphene with a large-size by sonication-free liquid-phase exfoliation of graphite with a new mechanism,” *Chemical Communications*, vol. 46, pp. 5091–5093, 2010.
- [40] X. Li, G. Zhang, X. Bai et al., “Highly conducting graphene sheets and Langmuir–Blodgett films,” *Nature Nanotechnology*, vol. 3, no. 9, pp. 538–542, 2008.
- [41] S. Vadukumpally, J. Paul, and S. Valiyaveettil, “Cationic surfactant mediated exfoliation of graphite into graphene flakes,” *Carbon*, vol. 47, no. 14, pp. 3288–3294, 2009.
- [42] J. C. Meyer, A. K. Geim, M. I. Katsnelson et al., “On the roughness of single- and bi-layer graphene membranes,” *Solid State Communications*, vol. 143, no. 1–2, pp. 101–109, 2007.
- [43] C. H. Park, L. Yang, Y. W. Son, M. Cohen, and S. Louie, “Anisotropic behaviours of massless Dirac fermions in graphene under periodic potentials,” *Nature Physics*, vol. 4, no. 3, pp. 213–217, 2008.
- [44] L. A. Ponomarenko, R. V. Gorbachev, G. L. Yu et al., “Cloning of Dirac fermions in graphene superlattices,” *Nature*, vol. 497, no. 7451, pp. 594–597, 2013.
- [45] N. Reckinger, E. Van Hooijdonk, F. Joucken, A. V. Tyurnina, S. Lucas, and J. F. Colomer, “Anomalous moiré pattern of graphene investigated by scanning tunneling microscopy: evidence of graphene growth on oxidized Cu(111),” *Nano Research*, vol. 7, no. 1, pp. 154–162, 2014.
- [46] X. J. He, H. B. Zhang, H. Zhang, X. J. Li, N. Xiao, and J. S. Qiu, “Direct synthesis of 3D hollow porous graphene balls from coal tar pitch for high performance supercapacitors,” *Journal of Materials Chemistry A*, vol. 2, no. 46, pp. 19633–19640, 2014.
- [47] C. Li, X. Zhang, K. Wang, H. T. Zhang, X. Z. Sun, and Y. W. Ma, “Three dimensional graphene networks for supercapacitor electrode materials,” *New Carbon Materials*, vol. 30, no. 3, pp. 193–206, 2015.
- [48] X. H. Xia, D. L. Chao, Y. Q. Zhang, Z. X. Shen, and H. J. Fan, “Three-dimensional graphene and their integrated electrodes,” *Nano Today*, vol. 9, no. 6, pp. 785–807, 2014.
- [49] Y. Ma and Y. Chen, “Three-dimensional graphene networks: synthesis, properties and applications,” *National Science Review*, vol. 2, no. 1, pp. 40–53, 2015.
- [50] Y. Xu, K. Sheng, C. Li, and G. Shi, “Self-assembled graphene hydrogel via a one-step hydrothermal process,” *ACS Nano*, vol. 4, no. 7, pp. 4324–4330, 2010.
- [51] Y. Zhang, Q. Zou, H. S. Hsu et al., “Morphology effect of vertical graphene on the high performance of supercapacitor electrode,” *ACS Applied Materials & Interfaces*, vol. 8, no. 11, pp. 7363–7369, 2016.

- [52] Y. Xu, G. Shi, and X. Duan, "Self-assembled three-dimensional graphene macrostructures: synthesis and applications in supercapacitors," *Accounts of Chemical Research*, vol. 48, no. 6, pp. 1666–1675, 2015.
- [53] A. K. Geim and I. V. Grigorieva, "Van der Waals heterostructures," *Nature*, vol. 499, no. 7459, pp. 419–425, 2013.
- [54] M. Garcia-Hernandez and J. Coleman, "Corrigendum: materials science of graphene: a flagship perspective," *2D Materials*, vol. 3, no. 1, p. 019501, 2016.
- [55] A. M. Maharramov, K. T. Mahmudov, M. N. Kopylovich, and A. J. L. Pompeiro, *Non-covalent Interactions in the Synthesis and Design of New Compounds*, John Wiley & Sons, Hoboken, NJ, USA, 2016.
- [56] Y. Hernandez, V. Nicolosi, M. Lotya et al., "High-yield production of graphene by liquid-phase exfoliation of graphite," *Nature Nanotechnology*, vol. 3, no. 9, pp. 563–568, 2008.
- [57] V. Nicolosi, M. Chhowalla, M. G. Kanatzidis, M. S. Strano, and J. N. Coleman, "Liquid exfoliation of layered materials," *Science*, vol. 340, no. 6139, p. 1226419, 2013.
- [58] U. Khan, H. Porwal, A. O'Neill, K. Nawaz, P. May, and J. N. Coleman, "Solvent-exfoliated graphene at extremely high concentration," *Langmuir*, vol. 27, no. 15, pp. 9077–9082, 2011.
- [59] A. V. Alaferdov, A. Gholamipour-Shirazi, M. A. Canesqui, Y. A. Danilov, and S. A. Moshkalev, "Size-controlled synthesis of graphite nanoflakes and multi-layer graphene by liquid phase exfoliation of natural graphite," *Carbon*, vol. 69, pp. 525–535, 2014.
- [60] J. Xu, D. K. Dang, V. T. Tran et al., "Liquid-phase exfoliation of graphene in organic solvents with addition of naphthalene," *Journal of Colloid and Interface Science*, vol. 418, pp. 37–42, 2014.
- [61] J. S. Park, L. Yu, C. S. Lee, K. Shin, and J. H. Han, "Liquid-phase exfoliation of expanded graphites into graphene nanoplatelets using amphiphilic organic molecules," *Journal of Colloid and Interface Science*, vol. 417, pp. 379–384, 2014.
- [62] E. Peng, E. S. G. Choo, P. Chandrasekharan et al., "Synthesis of manganese ferrite/graphene oxide nanocomposites for biomedical applications," *Small*, vol. 8, no. 23, pp. 3620–3630, 2012.
- [63] M. Marcaccio and F. Paolucci, *Making and Exploiting Fullerenes, Graphene, and Carbon Nanotubes*, Springer, Berlin, Heidelberg, 2014.
- [64] D. Datta, J. Li, N. Koratkar, and V. B. Shenoy, "Enhanced lithiation in defective graphene," *Carbon*, vol. 80, pp. 305–310, 2014.
- [65] D. Er, E. Detsi, H. Kumar, and V. B. Shenoy, "Defective graphene and graphene allotropes as high-capacity anode materials for Mg ion batteries," *ACS Energy Letters*, vol. 1, no. 3, pp. 638–645, 2016.
- [66] D. Datta, J. Li, and V. B. Shenoy, "Defective graphene as a high-capacity anode material for Na- and Ca-ion batteries," *ACS Applied Materials & Interfaces*, vol. 6, no. 3, pp. 1788–1795, 2014.
- [67] Z. Mao, H. Xu, and D. Wang, "Molecular mimetic self-assembly of colloidal particles," *Advanced Functional Materials*, vol. 20, no. 7, pp. 1053–1074, 2010.
- [68] K. Parvez, Z.-S. Wu, R. Li et al., "Exfoliation of graphite into graphene in aqueous solutions of inorganic salts," *Journal of the American Chemical Society*, vol. 136, no. 16, pp. 6083–6091, 2014.
- [69] X. Zhang, J. Zhang, Z. Liu, and C. Robinson, "Inorganic/organic mesostructure directed synthesis of wire/ribbon-like polypyrrole nanostructures," *Chemical Communications*, vol. 16, pp. 1852–1853, 2004.
- [70] X. Fan, Z. Yang, and N. He, "Hierarchical nanostructured polypyrrole/graphene composites as supercapacitor electrode," *RSC Advances*, vol. 5, no. 20, pp. 15096–15102, 2015.
- [71] S. U. Pickering, "CXCVI.—emulsions," *Journal of the Chemical Society, Transactions*, vol. 91, pp. 2001–2021, 1907.
- [72] S. D. Berger, D. R. McKenzie, and P. J. Martin, "EELS analysis of vacuum arc-deposited diamond-like films," *Philosophical Magazine Letters*, vol. 57, no. 6, pp. 285–290, 1988.
- [73] Z. S. Wu, W. Ren, L. Gao, B. Liu, C. Jiang, and H. M. Cheng, "Synthesis of high-quality graphene with a pre-determined number of layers," *Carbon*, vol. 47, no. 2, pp. 493–499, 2009.
- [74] P. Le Doussal and L. Radzihovsky, "Self-consistent theory of polymerized membranes," *Physical Review Letters*, vol. 69, no. 8, pp. 1209–1212, 1992.
- [75] D. R. Nelson, T. Piran, and S. Weinberg, *Statistical Mechanics of Self-Avoiding Manifolds (Part II)*, World Scientific, Singapore, 2004.
- [76] C. J. Shih, A. Vijayaraghavan, R. Krishnan et al., "Bi- and trilayer graphene solutions," *Nature Nanotechnology*, vol. 6, no. 7, pp. 439–445, 2011.
- [77] K. Kim, Z. Lee, B. D. Malone et al., "Multiply folded graphene," *Physical Review B*, vol. 83, Article ID 245433, 8 pages, 2011.



Hindawi

Submit your manuscripts at
www.hindawi.com

